Astron. & Astrophys. 49, 103 – 106 (1976)

Vibrational Stability towards Non-radial Oscillations during Central Hydrogen Burning

A. Noels, A. Boury, M. Gabriel and R. Scuflaire
Institut d'Astrophysique de l'Université de Liège

Received November 10, 1975, revised January 22, 1976

Summary. Vibrational stability towards low order g^+ modes ($l=1$) have been tested in the case of three evolutionary sequences corresponding to 0.5, 0.6 and 1.1 $M_\odot$. The instability detected in the solar case and associated with an evolution with recurrent mixing and thermal imbalance phases, is also present in 0.5 and 0.6 $M_\odot$. On the other hand, all models of 1.1 $M_\odot$ are stable. The presence of a convective core in stars more massive than 1 $M_\odot$ fixes to that value the upper boundary of the range of mass concerned by this instability.

Key words: non-radial oscillations — vibrational stability

I. Introduction

The study of vibrational stability towards non-radial oscillations has recently received renewed interest. In particular, it raised hopes to bring a solution to the problem of the apparent absence of solar neutrinos in Davis' experiment. Fowler (1972) suggested that this absence could be the consequence of the sun's being in a phase of readjustment following a fast mixing of the core. This mixing could have been produced by a vibrational instability towards low g^+ modes (Dilke and Gough, 1972). That a solar mass star becomes vibrationally unstable during central hydrogen burning was shown in several works (Christensen-Dalsgaard *et al.*, 1974, 1975; Noels *et al.*, 1975; Boury *et al.*, 1975; Shibahashi *et al.*, 1975). A chemically homogeneous 0.5 $M_\odot$ star is also unstable towards low g^+ modes (Noels *et al.*, 1974). Therefore one can suspect that all non fully convective stars with masses lower than about 1 $M_\odot$ would be unstable towards g^+ modes during part of the main sequence phases. This instability could still persist in masses slightly larger where the convective core remains small. To check these points we have extended our previous calculations for the 0.5 $M_\odot$ star and we have tested the stability of a 0.6 $M_\odot$ and a 1.1 $M_\odot$ star. The analysis shows that the two lower masses are indeed unstable during an important fraction of the main sequence phase and that, as in the sun, the instability is driven by the nuclear reactions. The 1.1 $M_\odot$ star is however already stable in the whole main-sequence phase: the instability thus disappears for stars only slightly more massive than the Sun.

If, as Dilke and Gough (1972) proposed, the vibrational instability triggers a mixing of the stellar core, the evolution will be different from the standard core for the range of unstable masses. In that range, the shape of the theoretical isochrones of old clusters as well as the star distribution on these isochrones will be modified. Their comparison could help to check Dilke and Gough's suggestion.

II. Models

Three evolutionary sequences corresponding to 0.5, 0.6 and 1.1 $M_\odot$ stars were computed with a Henyey method (without any mixing in the radiative parts) from the gravitational contraction to the exhaustion of hydrogen at the centre. The chemical composition was chosen as follows: $X=0.602$, $Z=0.044$ for 0.6 and 1.1 $M_\odot$ and $X=0.9$, $Z=0.001$ for 0.5 $M_\odot$. Properties of the models involved in the stability analysis are given in Table 1, where q_e and q_c mean respectively the mass fraction at the inner limit of the convective envelope and at the upper limit of the convective core; all other symbols have their usual meaning.

Less evolved models of 0.5 $M_\odot$ were known, from a previous study (Noels *et al.*, 1974), to be unstable towards low g^+ modes so they were not included. Model 1, in the sequence of 0.6 $M_\odot$ was also studied in Noels *et al.* (1974). The instability detected in that later case was however very marginal. Since several improvements have been made in the theory as well as in the computational method (see Boury *et al.*, 1975), it was necessary to resume the stability calculations.

III. Vibrational Stability

All details concerning the equations and the method used to determine the adiabatic frequences, σ_a(= Period/2π) of non-radial oscillations can be found in Boury *et al.*

Table 1. Properties of the evolutionary models corresponding to $0.5\,M_\odot$, $0.6\,M_\odot$ and $1.1\,M_\odot$

Model number	Age	T_c	ϱ_c	$\varrho_c/\bar{\varrho}$	X_c/X_{surf}	L	$\log T_e$	q_e	q_f
$0.5\,M_\odot$									
1	8.126 (10)	1.003 (7)	2.252 (2)	30.17	0.289	2.459 (32)	3.6341	0.737	—
2	1.021 (11)	1.108 (7)	3.583 (2)	61.07	0.156	2.933 (32)	3.6360	0.804	—
3	1.092 (11)	1.159 (7)	4.354 (2)	82.70	0.117	3.189 (32)	3.6372	0.825	—
$0.6\,M_\odot$									
1	2.857 (8)	1.069 (7)	9.685 (1)	21.67	0.993	3.883 (32)	3.6334	0.894	—
2	1.326 (10)	1.135 (7)	1.411 (2)	39.58	0.626	4.921 (32)	3.6428	0.898	—
3	1.967 (10)	1.212 (7)	1.886 (2)	60.48	0.448	5.770 (32)	3.6506	0.906	—
4	2.288 (10)	1.262 (7)	2.242 (2)	77.85	0.360	6.332 (32)	3.6547	0.910	—
$1.1\,M_\odot$									
1	2.113 (7)	1.547 (7)	7.293 (1)	62.89	0.999	5.816 (33)	3.7856	0.994	0.111
2	2.704 (7)	1.580 (7)	8.189 (1)	74.80	0.998	6.317 (33)	3.7907	0.996	0.065
3	1.251 (8)	1.705 (7)	1.065 (2)	98.56	0.974	7.249 (33)	3.8045	0.999	0.030
4	6.068 (8)	1.761 (7)	1.156 (2)	116.8	0.846	7.662 (33)	3.8044	0.999	0.039
5	1.192 (9)	1.827 (7)	1.281 (2)	145.5	0.668	8.089 (33)	3.8017	0.999	0.045
6	1.877 (9)	1.921 (7)	1.490 (2)	199.0	0.418	8.479 (33)	3.7952	0.998	0.049

Numbers in parentheses indicate the power of 10 which multiplies the preceding numbers.

Table 2. Periods of the adiabatic oscillations and vibrational stability (see text)

Model	$l=1$	P(s)	σ^{-1}(y)[a]	σ'_N(y^{-1})	σ'_F(y^{-1})	Model	$l=1$	P(s)	σ^{-1}(y)[a]	σ'_N(y^{-1})	σ'_F(y^{-1})
$0.5\,M_\odot$						$0.6\,M_\odot$					
1	g_1	2.828(3)	−3.79(7)	4.77(−8)	2.13(−8)	4	g_1	3.009(3)	4.04(7)	8.63(−8)	1.11(−7)
	g_2	3.942(3)	−7.76(7)	5.87(−8)	4.59(−8)		g_2	4.131(3)	4.77(7)	9.87(−8)	1.20(−7)
	g_3	5.129(3)	5.90(7)	6.11(−8)	7.81(−8)		g_3	5.267(3)	1.14(7)	1.08(−7)	2.07(−8)
	g_4	6.303(3)	1.82(7)	6.02(−8)	1.15(−7)		g_4	6.337(3)	5.94(6)	9.37(−8)	2.62(−7)
2	g_1	2.274(3)	−2.43(8)	4.36(−8)	3.95(−8)	$1.1\,M_\odot$					
	g_2	3.068(3)	−1.23(8)	5.79(−8)	4.97(−8)	1	g_1	6.887(3)	4.32(6)	1.24(−7)	3.56(−7)
	g_3	3.952(3)	3.56(7)	6.40(−8)	9.21(−8)		g_2	1.020(4)	2.02(6)	2.18(−7)	7.16(−7)
	g_4	4.837(3)	1.34(7)	6.43(−8)	1.39(−7)		g_3	1.353(4)	9.87(5)	3.09(−7)	1.32(−6)
3	g_1	2.133(3)	7.71(6)	3.85(−8)	1.68(−7)		g_4	1.698(4)	5.55(5)	4.05(−7)	2.21(−6)
	g_2	2.802(3)	1.78(7)	5.72(−8)	6.28(−8)	2	g_1	6.426(3)	4.46(6)	1.85(−7)	4.10(−7)
	g_3	3.508(3)	2.99(7)	6.52(−8)	9.88(−8)		g_2	9.458(3)	2.66(6)	3.47(−7)	7.23(−7)
$0.6\,M_\odot$							g_3	1.244(3)	1.26(6)	5.06(−7)	1.30(−6)
1	g_1	5.780(3)	1.94(7)	5.84(−7)	6.35(−7)		g_4	1.548(4)	6.85(5)	6.39(−7)	2.10(−6)
	g_2	8.280(3)	−9.77(8)	1.53(−7)	1.52(−7)	3	g_1	5.633(3)	4.15(6)	3.66(−7)	6.07(−7)
	g_3	1.108(4)	2.75(7)	2.19(−7)	2.55(−7)		g_2	8.106(3)	5.66(6)	6.23(−7)	7.99(−7)
	g_4	1.414(4)	7.15(6)	2.47(−7)	3.87(−7)		g_3	1.049(4)	1.83(6)	7.77(−7)	1.33(−6)
2	g_1	4.088(3)	−3.17(7)	1.13(−7)	8.19(−8)		g_4	1.293(4)	8.96(5)	8.82(−7)	2.00(−6)
	g_2	5.610(3)	8.66(7)	8.43(−8)	9.59(−8)	4	g_1	5.232(3)	2.50(6)	5.81(−7)	9.81(−7)
	g_3	7.034(3)	1.67(7)	9.23(−8)	1.52(−7)		g_2	6.885(3)	8.72(6)	7.44(−7)	8.58(−7)
	g_4	8.577(3)	7.49(6)	1.02(−7)	2.36(−7)	5	g_1	4.284(3)	3.34(6)	5.07(−7)	3.05(−5)
3	g_1	3.526(3)	−4.93(7)	1.03(−7)	8.30(−8)		g_2	5.944(3)	2.06(6)	2.64(−7)	7.50(−6)
	g_2	4.610(3)	6.20(7)	9.48(−8)	1.11(−7)		g_3	8.157(3)	2.54(6)	3.00(−7)	6.95(−7)
	g_3	5.834(3)	1.31(7)	8.99(−8)	1.66(−7)		g_4	1.035(4)	1.33(6)	3.02(−7)	5.24(−7)
	g_4	7.020(3)	6.57(6)	9.31(−8)	2.45(−7)	6	g_1	4.529(3)	7.62(3)	9.16(−9)	1.32(−4)
							g_2	5.645(3)	6.24(5)	2.36(−7)	1.84(−6)

[a]) a negative sign means instability.

(1975). The periods corresponding to $l=1$, l being as usual the degree of the spherical surface harmonic, are listed in Table 2 for the first g^+ modes. The two main features observed in the behaviour of the eigenfunctions in the case of the $1\,M_\odot$ models are again apparent. First, for a given mode, the absolute value of the amplitude of $\delta p/p$ at the surface increases with $\varrho_c/\bar{\varrho}$, when compared to its values at the first extremum. Second, the nodes come closer and closer to the centre as the evolution proceeds.

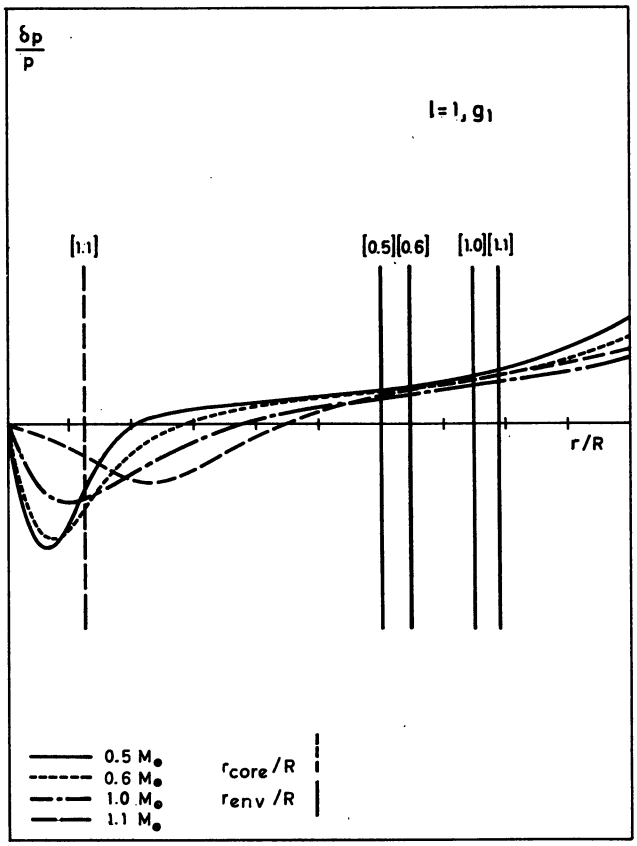

Fig. 1. $\delta p/p$ as a function of r/R in the case $l=1$, g_1 (———: model 2, 0.5 $M_\odot$; ·····: model 3, 0.6 $M_\odot$; –·–·–: model 3, 1 $M_\odot$; – – – – –: model 1, 1.1 $M_\odot$). Scale is such that $\int_0^M |\delta r|^2 dm = \frac{MR^2}{4\pi}$

However the presence of convective zones introduces some differences between the three cases. Inside the radius r_0 such that

$$\sigma_a^2 = \left[\frac{\Gamma_1 p l(l+1)}{\varrho r^2}\right]_{r=r_0} \quad (1)$$

the amplitude of a g^+ mode oscillates (spatially) in radiative zones (Scuflaire, 1974). In ZAMS stars, r_0/R is close to the surface and smaller of larger values of $\varrho_c/\bar{\varrho}$. For a given mass, as evolution proceeds, r_0 decreases. Outside r_0, the amplitude can oscillate (spatially) even in convective regions as long as the frequency of pulsation is larger than the Brunt-Väisälä frequency. Thus, for values of $\varrho_c/\bar{\varrho}$ low enough, all the nodes, except sometimes one, will be found in the radiative zone. It follows that, because of the growth of the convective envelope, the position of the first node, for a given $\varrho_c/\bar{\varrho}$, moves closer to the centre as the mass of the star decreases. In the opposite way the presence of a convective core in the 1.1 $M_\odot$ star keeps the first node farther from the centre. The illustration of this is given in Fig. 1 where $\delta p/p$ corresponding to the $l=1$, g_1 mode is plotted as a function of $x(=r/R)$ for the model which for each mass has $\varrho_c/\bar{\varrho}$ about 60. The limits of the convective zones are also indicated on the x-axis.

The influence of the non-adiabatic terms is evaluated as usual through the damping coefficient

$$\sigma' = \sigma'_F - \sigma'_N$$

with the flux part

$$\sigma'_F \equiv \int_0^{M_a} \frac{\delta T}{T} \delta\left(\frac{1}{\varrho}\nabla\cdot\boldsymbol{F}\right) dm \Big/ \left(2\sigma_a^2 \int_0^M \boldsymbol{\delta r}\cdot\boldsymbol{\delta r}^* dm\right)$$

and the nuclear part

$$\sigma'_N \equiv \int_0^{M_a} \frac{\delta T}{T} \delta\varepsilon dm \Big/ \left(2\sigma_a^2 \int_0^M \boldsymbol{\delta r}\cdot\boldsymbol{\delta r}^* dm\right)$$

where the symbol δ refers to lagrangian perturbations and σ' is calculated in terms of the adiabatic solutions. The limit of integration is set at mass M_a where the non adiabatic correction to $\delta T/T$ becomes equal to the adiabatic value. The development of σ'_F and its behaviour which is the same in the present models as in the solar evolution are given in Boury *et al.* (1975) σ'_F is globally stabilizing. σ'_N is of course, destabilizing but, in the competition with σ'_F in Eq. (1) the importance of the nuclear driving strongly depends on the relative location of the first node of $\delta p/p$ with respect to the distribution of the nuclear energy generation ε. If, in the course of evolution, this distribution remained unchanged, the progressive displacement of the node closer to the centre but still sufficiently outside the energy generation region would favour the driving. When the node reaches that region, the effect is reversed.

Things become more intricate when the change in profile of the energy generation distribution is taken into account. In the 1.1 $M_\odot$ evolution, because of the chemical discontinuity at the edge of the convective core in models 4 to 6, the ratio of the hydrogen abundances on the inner and outer sides of the core boundary decreases from 0.83 in model 5 to 0.58 in model 6. It follows that, although ε remains largest at the centre, there exists a secondary maximum of increasing magnitude, with which, for modes $l=1$, g_1 and g_2, a maximum of amplitude (in absolute value) of $\delta p/p$ comes into coincidence. This effect however is weakened by the decrease outwards of v_e, the effective sensitivity of nuclear reactions to temperature which in model 5 is ~ 16 in the core due to the importance of the CNO cycle but falls to ~ 10 just outside the core because of the dominance of the $p-p$ chain [Eq. (22) in Boury *et al.*, 1975]. In all models of the 1.1 $M_\odot$ sequence, the maximum of $\delta p/p$ is always outside the convective core. Amplitudes are low where ε is significant and the nuclear driving is small. All models are thus stable. In the 0.5 $M_\odot$, a feature to notice is that the maximum of ε is no longer located at the centre in the evolved models analyzed here (see Fig. 2) which reinforces σ'_N.

If the presence of a convective core is a stabilizing factor, an extended convective envelope, on the contrary, favours the instability as it keeps the amplitude smaller in the outer layers and lessens σ'_F. All other things being

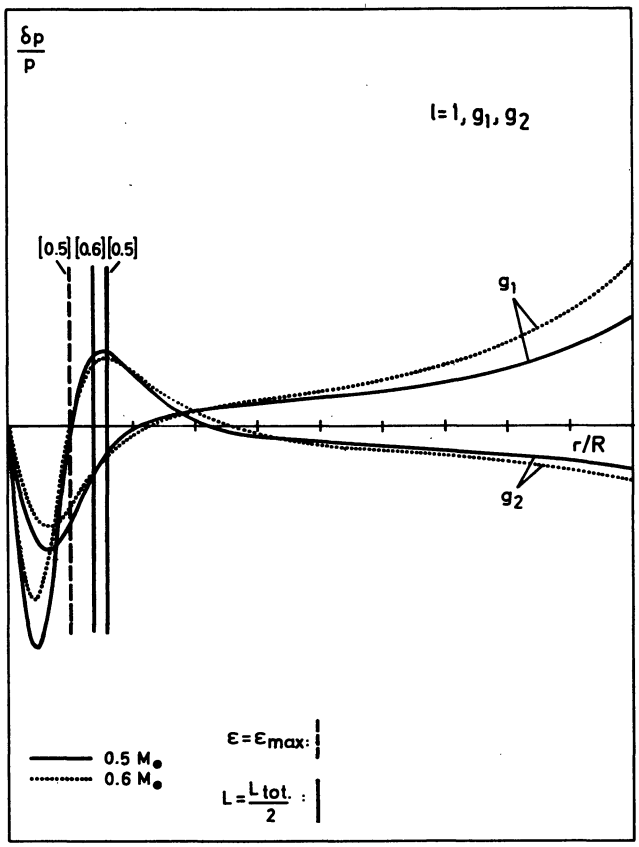

Fig. 2. $\delta p/p$ as a function of r/R in the cases $l=1$, g_1 and $l=1$, g_2 (———: model 2, 0.5 $M_\odot$; · · · · ·: model 3, 0.6 $M_\odot$). Scale as in Fig. 1

equal, the instability is thus favoured in the 0.5 $M_\odot$ star compared to the 0.6 $M_\odot$ star. For comparable $\varrho_c/\bar{\varrho}$, the $l=1$, g_2 mode is still unstable in 0.5 $M_\odot$ but has become stable again in 0.6 $M_\odot$.

It must be said however that details are complicated, depending, among other things, on the behaviour of the opacity and, as said above, on the distribution of ε relative to the amplitudes of the eigenfunctions. For example, as was already observed in the case of the sun, the modes best appropriate to an instability in a little evolved model are those of $l=1$ and among them, g_1, g_2, g_3 etc. in decreasing order. But in model 1 of 0.6 $M_\odot$, the model $l=1$, g_2 is slightly unstable while the g_1 mode is not. This is due to the more favourable position of the maximum of $\delta p/p$ in the former mode. A similar comparison can be made between the 0.6 $M_\odot$ star where, in models 2 and up, the g_2 mode is stable while, in the sun, it is unstable.

Anyway in all cases, the increase of $\varrho_c/\bar{\varrho}$ during the evolution eventually renders the amplitudes in the outer layers great enough to restore stability for all modes (see Gabriel *et al.*, 1975). As this important increase in amplitude first affects the g_1 mode, the relative stability of different modes changes. The g_1 mode becomes more stable than the g_2 and even higher modes. For higher $\varrho_c/\bar{\varrho}$ values, the same behaviour is observed for the g_2 mode and so on.

IV. Conclusions

The instability observed in the case of 1 $M_\odot$ is also found in less massive (0.5 and 0.6 $M_\odot$) at least for the mode $l=1$, g_1. This instability is essentially of the same nature as the one discussed in the solar case but is enhanced, on the one hand, by the presence of a convective envelope and on the other hand (in 0.5 $M_\odot$ only) by the fact that the maximum of the nuclear energy production rate is no longer at the centre for the models under scope. In the two cases, stabilization is restored for values of $\varrho_c/\bar{\varrho}$ between 70 and 80.

The range of masses concerned by this instability does not extend far beyond 1 $M_\odot$ because the appearance of a convective core in more massive stars is a strongly stabilizing factor; all models of 1.1 $M_\odot$ studied here are stable. As far as the theoretical isochrones appropriate to the age determination of globular clusters are concerned, the modifications introduced by this instability depend on the assumptions made as to its consequences concerning a possible mixing. If every star of mass intermediate between 0.5 and 1 $M_\odot$ passes through the hydrogen burning phases with mixing in a fraction of the total mass, the fitting of observational H–R diagrams of old clusters with theoretical isochrones must be reconsidered. This may furnish a new test for Dilke and Gough's suggestion.

References

Boury, A., Gabriel, M., Noels, A., Scuflaire, R., Ledoux, P. 1975, *Astron. & Astrophys.* **41**, 279

Christensen-Dalsgaard, J., Dilke, F. W. N., Gough, D. O. 1974, *Monthly Notices Roy. Astron. Soc.* **169**, 429

Christensen-Dalsgaard, J., Gough, D. O. 1975, Hydrodynamic Phenomena in Stellar Evolution, XIX Liège Symposium, *Mém. Soc. Roy. Sc. Lg.* 6th series, **8**, 309

Dilke, F. W. N., Gough, D. O. 1972, *Nature* **240**, 262

Fowler, W. A. 1972, *Nature* **238**, 24

Gabriel, M., Scuflaire, R., Noels, A., Boury, A. 1975, *Astron. & Astrophys.* **40**, 33

Noels, A., Boury, A., Scuflaire, R., Gabriel, M. 1974, *Astron. & Astrophys.* **31**, 185

Noels, A., Gabriel, M., Boury, A., Scuflaire, R., Ledoux, P. 1975, Hydrodynamic Phenomena in Stellar Evolution, XIX Liège symposium, *Mem. Soc. Roy. Sc. Lg.* 6th series, **8**, 317

Scuflaire, R. 1974, *Astron. & Astrophys.* **34**, 449

Shibahashi, H., Osaki, Y., Unno, W. 1975, preprint

A. Noels
A. Boury
M. Gabriel
R. Scuflaire
Institut d'Astrophysique
5, avenue de Cointe
4200 Cointe-Ougrée, Belgium